nature medicine

Donor CD19 CAR T cells exert potent graft-versus-lymphoma activity with diminished graft-versus-host activity

Arnab Ghosh[1,7], Melody Smith[1,7], Scott E James[1,2,7], Marco L Davila[2,6,7], Enrico Velardi[1], Kimon V Argyropoulos[1], Gertrude Gunset[2], Fabiana Perna[2], Fabiana M Kreines[1], Emily R Levy[1], Sophie Lieberman[1], Hillary V Jay[1], Andrea Z Tuckett[1], Johannes L Zakrzewski[3], Lisa Tan[1], Lauren F Young[1], Kate Takvorian[1], Jarrod A Dudakov[1,6], Robert R Jenq[1], Alan M Hanash[1], Ana Carolina F Motta[4,6], George F Murphy[4], Chen Liu[5], Andrea Schietinger[1], Michel Sadelain[1,2,7] & Marcel R M van den Brink[1,2,7]

Allogeneic hematopoietic stem cell transplantation (allo-HSCT) is a potentially curative therapy for hematological malignancies. However, graft-versus-host disease (GVHD) and relapse after allo-HSCT remain major impediments to the success of allo-HSCT. Chimeric antigen receptors (CARs) direct tumor cell recognition of adoptively transferred T cells[1–5]. CD19 is an attractive CAR target, which is expressed in most B cell malignancies, as well as in healthy B cells[6,7]. Clinical trials using autologous CD19-targeted T cells have shown remarkable promise in various B cell malignancies[8–15]. However, the use of allogeneic CAR T cells poses a concern in that it may increase risk of the occurrence of GVHD, although this has not been reported in selected patients infused with donor-derived CD19 CAR T cells after allo-HSCT[16,17]. To understand the mechanism whereby allogeneic CD19 CAR T cells may mediate anti-lymphoma activity without causing a significant increase in the incidence of GVHD, we studied donor-derived CD19 CAR T cells in allo-HSCT and lymphoma models in mice. We demonstrate that alloreactive T cells expressing CD28-costimulated CD19 CARs experience enhanced stimulation, resulting in the progressive loss of both their effector function and proliferative potential, clonal deletion, and significantly decreased occurrence of GVHD. Concurrently, the other CAR T cells that were present in bulk donor T cell populations retained their anti-lymphoma activity in accordance with the requirement that both the T cell receptor (TCR) and CAR be engaged to accelerate T cell exhaustion. In contrast, first-generation and 4-1BB-costimulated CAR T cells increased the occurrence of GVHD. These findings could explain the reduced risk of GVHD occurring with cumulative TCR and CAR signaling.

To evaluate the impact of CAR signaling on both the anti-lymphoma and GVHD activities of allogeneic T cells, we constructed a panel of retroviral vectors encoding CARs targeting mouse CD19 (**Fig. 1a**): mouse-1928z (m1928z) CAR encodes mouse CD28 linked to CD3ζ endodomains and is specific for mouse CD19 (ref. 18); m19delta lacks the CD3ζ signaling domain, enabling it to serve as a non-signaling, control CAR; m19z lacks a costimulatory signal; m19BBz encodes mouse 4-1BB and CD3ζ endodomains; hum1928z contains a human-CD19-specific single-chain variable fragment (scFv) and does not cross-react with mouse CD19; and m19delta.GFP and m1928z.GFP encode GFP fusion proteins[13]. We verified CAR expression by cells using flow cytometry (**Supplementary Fig. 1**), and m1928z, but not m19delta, T cells specifically lysed CD19-expressing syngeneic targets (**Fig. 1b**). In a major histocompatibility complex (MHC)-disparate model of allo-HSCT (B6→BALB/c), we compared m1928z and m19delta T cells in mice inoculated with A20-TGL B cell lymphoma cells to model lymphoma relapse. Every recipient from each group of the allogeneic m19delta T cells developed lethal, acute GVHD, whereas recipients of only T cell–depleted bone marrow (BM) allografts died of lymphoma.Strikingly, the recipients of m1928z T cells exhibited reduced tumor growth and reduced mortality due to GVHD, resulting in a significantly improved overall survival rate, in comparison to mice treated with m19delta T cells and untreated controls ($P < 0.0001$; **Fig. 1c**,**d** and **Supplementary Fig. 2**). When we treated the BALB/c recipients of B6 BM that were infused with A20-TGL cells with varying doses of m1928z T cells, we found a dose-dependent increase in the survival rate of the BALB/c mice (**Fig. 1e**), demonstrating increasing anti-lymphoma activity without increased occurrence of GVHD when the T cell dosages ranged from 0.125–0.5 $\times 10^6$ cells per mouse.Transfer of at least 0.5 $\times 10^6$ m1928z T cells into BALB/c mice was required to promote anti-lymphoma activity

[1]Department of Medicine and Immunology Program, Memorial Sloan Kettering Cancer Center, New York, New York, USA. [2]Center of Cell Engineering, Memorial Sloan Kettering Cancer Center, New York, New York, USA. [3]Pediatrics, Memorial Sloan Kettering Cancer Center, New York, New York, USA. [4]Program in Dermatopathology, Department of Pathology, Brigham and Women's Hospital and Harvard Medical School, Boston, Massachusetts, USA. [5]Department of Pathology and Laboratory Medicine, Rutgers–Robert Wood Johnson Medical School, Newark, New Jersey, USA. [6]Present addresses: Department of Blood and Marrow Transplantation, H. Lee Moffitt Cancer Center and Research Institute, Tampa, Florida, USA (M.L.D.), Program in Immunology, Clinical Research Division, Fred Hutchinson Cancer Research Center, Seattle, Washington, USA (J.A.D.) and University of São Paulo, São Paulo, Brazil (A.C.F.M.). [7]These authors contributed equally to this work. Correspondence should be addressed to M.R.M.v.d.B. (vandenbm@mskcc.org) or M.S. (sadelaim@mskcc.org).

Received 13 October 2016; accepted 7 November 2016; published online 9 January 2017; doi:10.1038/nm.4258

beyond the level conferred by the alloreactive graft-versus-lymphoma (GVL) effect that was mediated by m19delta T cells (**Supplementary Fig. 3**).

We confirmed the diminished GVHD-inducing activity of m1928z T cells in allo-HSCT recipients by evaluating the survival and clinical GVHD scores of recipients in the absence of tumors (**Fig. 1f**). We performed experiments in acute GVHD models comprising MHC-disparate (B6→BALB/c)[19] and MHC-haploidentical (B6→CBF1)[20] combinations to determine whether the inhibition of GVHD by m1928z T cells was consistent in mice with different genetic backgrounds and with heterogeneous alloreactive TCR antigen specificities. Histopathological analyses showed that GVHD scores were significantly lower in the major target organs for GVHD (skin, liver, and small and large intestines) in allo-HSCT recipients of m1928z T cells when compared with recipients of m19delta T cells in both transplant models (**Fig. 1g**). However, when we gave recipients very high doses of T cells (10^7 cells per mouse), we noted increased mortality rates in both m1928z and m19delta T cell recipients (**Supplementary Fig. 4**), indicating that the transfer of large numbers of non-transduced T cells was sufficient to promote comparable levels of GVHD in recipients of m1928z and m19delta T cells. Our findings suggest that GVHD in m1928z T cell recipients may occur as a result of either (i) a high number of non-transduced cells mediating GVHD or (ii) excess alloreactive m1928z T cells that direct their effector function toward GVHD target organs in the setting of limited numbers of B cells. Notably, our findings argue against the existence of a mechanism in which alteration of the host environment—for example, through B cell depletion by m1928z T cells—dominantly inhibits the occurrence of GVHD. These data are of relevance because current clinical protocols for CAR T cells do not involve post-transduction sorting and, in addition to the cytokine release syndrome seen when high doses of CAR T cells are administered, there is an increased risk of GVHD arising when transferring greater numbers of non-transduced cells[21].

Despite the decreased occurrence of GVHD, the bulk m1928z T cell population maintained anti-CD19 activity *in vivo*, as demonstrated by the persistent B cell aplasia present in allo-HSCT recipients of m1928z T cells (**Fig. 2a**) and the observation that m1928z T cells were present at least 60 d after HSCT (**Fig. 2b**). Additionally, m1928z T cells harvested from adoptively transferred mice mediated *ex vivo* anti-CD19 lytic activity (**Fig. 2c**). To study alloreactive CD19 CAR T cell activity over a more prolonged time frame, we analyzed m1928z T cell activity against normal B cells in a model of chronic GVHD (B6→B10.BR), observing reduced intestinal pathology and attenuated lethality (**Supplementary Fig. 5a**), in comparison with models of acute GVHD[22]. m1928z T cells again promoted reduced occurrence of GVHD in recipients in this model but also mediated severe B cell aplasia when compared with m19delta T cells, which resulted in GVHD and concomitant mild alloreactivity-related B cell depletion in the peripheral blood of recipients (**Supplementary Fig. 5b**). Histopathological analyses demonstrated loss of B cell follicles, as well as loss of $B220^+$ follicular B cells, in recipients of m1928z T cells when compared to recipients of either m19delta T cells or BM only (**Fig. 2d**).

We hypothesized that the decreased potential of m1928z T cells to cause GVHD resulted from cumulative CAR and alloreactive TCR signaling, leading to exhaustion and eventual deletion of the alloreactive CAR T cells while the non-alloreactive CAR T cells retained activity against $CD19^+$ targets. To test this hypothesis, we first assessed the *in vivo* expansion and distribution of donor T cells by infusing BALB/c recipients with luciferase-expressing B6 m1928z or m19delta T cells. Bioluminescence imaging showed significantly reduced expansion of m1928z T cells when compared to m19delta T cells in BALB/c recipients (**Fig. 3a**). Additionally, there were fewer splenic donor $CD8^+$ T cells in recipients of m1928z versus m19delta T cells 7 d after HSCT (**Supplementary Fig. 6a**). GVHD target organs and lymph nodes also exhibited fewer $Thy1.1^+$ donor m1928z T cells than m19delta T cells (**Fig. 3b**). Splenocytes isolated 14 d after HSCT displayed a reduced frequency of $Thy1.1^+$ donor T cells expressing the gut homing markers CCR5 and L-PAM in recipients of m1928z versus m19delta T cells (**Fig. 3c**). Further T cell immunophenotypic analyses showed significantly fewer activated and effector memory $CD8^+$ T cells in the spleens of mice receiving m1928z versus m19delta T cells 7 d after transplantation (**Supplementary Fig. 6b**). No differences in T cell polarization were identified in studies analyzing the expression of transcription factors specific for T helper type 1 (T_H1; T-bet), T helper type 2 (T_H2; GATA-3), or regulatory T (Foxp3) cells in splenocytes (**Supplementary Fig. 6c**). We also found that there were significantly lower levels of interferon (IFN)-γ, tumor necrosis factor (TNF)-α, and IL-6 in sera from the BALB/c recipients of B6 m1928z versus m19delta T cells 7 d after HSCT (**Fig. 3d**). We investigated whether a high burden of malignant $CD19^+$ cells might enhance m1928z T cell cytokine production and activation, which could phenocopy cytokine release syndrome and exacerbate GVHD. In a modification of the B6→BALB/c model that included establishment of A20-TLG lymphoma before transplantation, we identified lower serum levels of granulocyte macrophage colony-stimulating factor (GM-CSF), IFN-γ, IL-6, and TNF-α in recipients of m1928z versus m19delta T cells (**Supplementary Fig. 7**). These data suggest that both the reduced proliferation (**Fig. 3a**) and *ex vivo* recovery (**Fig. 3b** and **Supplementary Fig. 6a**) of m1928z T cells when compared with m19delta T cells result in the presence of fewer functional T cells to elaborate cytokines in response to lymphoma cells *in vivo*. Notably, our data are in disagreement with a model in which enhanced cytokine secretion by m1928z CAR T cells in response to lymphoma cells promotes GVHD or cytokine-release-mediated lethality, as was seen in a recent mouse study[23]. Possible reasons for this difference include intrinsic structural differences in the CAR constructs, which can influence the survival and activity of CAR T cells in response to antigen challenge[24].

To assess the contribution of the alloreactive TCR to the decreased occurrence of GVHD, we took advantage of a transgenic GVHD model in which donor T cells are obtained from *Rag1*-knockout mice transgenic for the ABM (monoclonal) TCR and target the allelic MHC class II molecule I-A^{bm12} expressed by B6.C-$H2^{bm12}$ (BM12) recipients. Transfer of ABM T cells is sufficient to cause GVHD in BM12 recipients, as well as BM12 allo-HSC graft rejection in immunodeficient mice[25]. We observed that GVHD occurred at a significantly lower frequency in the allo-HSCT BM12 recipients of ABM m1928z versus m19delta T cells (**Fig. 3e**). When combined with the above results demonstrating reduced proliferation and cytokine production of m1928z versus m19delta T cells, this finding further compounds evidence of a model where m1928z T cells develop functional exhaustion in allogeneic hosts.

To investigate the role of costimulatory signals in the case of CAR-mediated protection from GVHD, we compared first-generation m19z T cells lacking enforced costimulation with CD28-costimulated m1928z T cells (**Fig. 1a**) in the B6→BALB/c GVHD model (**Fig. 3f**). Treatment with m19z T cells resulted in a significantly higher rate of GVHD-induced mortality than treatment with m1928z T cells (although the mortality rate was less than that caused by m19delta T cells),

suggesting that enforced costimulation affects the strength of protection from GVHD. As different CARs have been shown to promote the development of exhaustion in response to repetitive CAR signaling[26,27], we compared m19BBz T cells with m1928z T cells (**Figs. 1a** and **3g**). Donor B6 m19BBz T cells mediated GVHD that was significantly more lethal than that seen with m1928z T cells, resulting in a

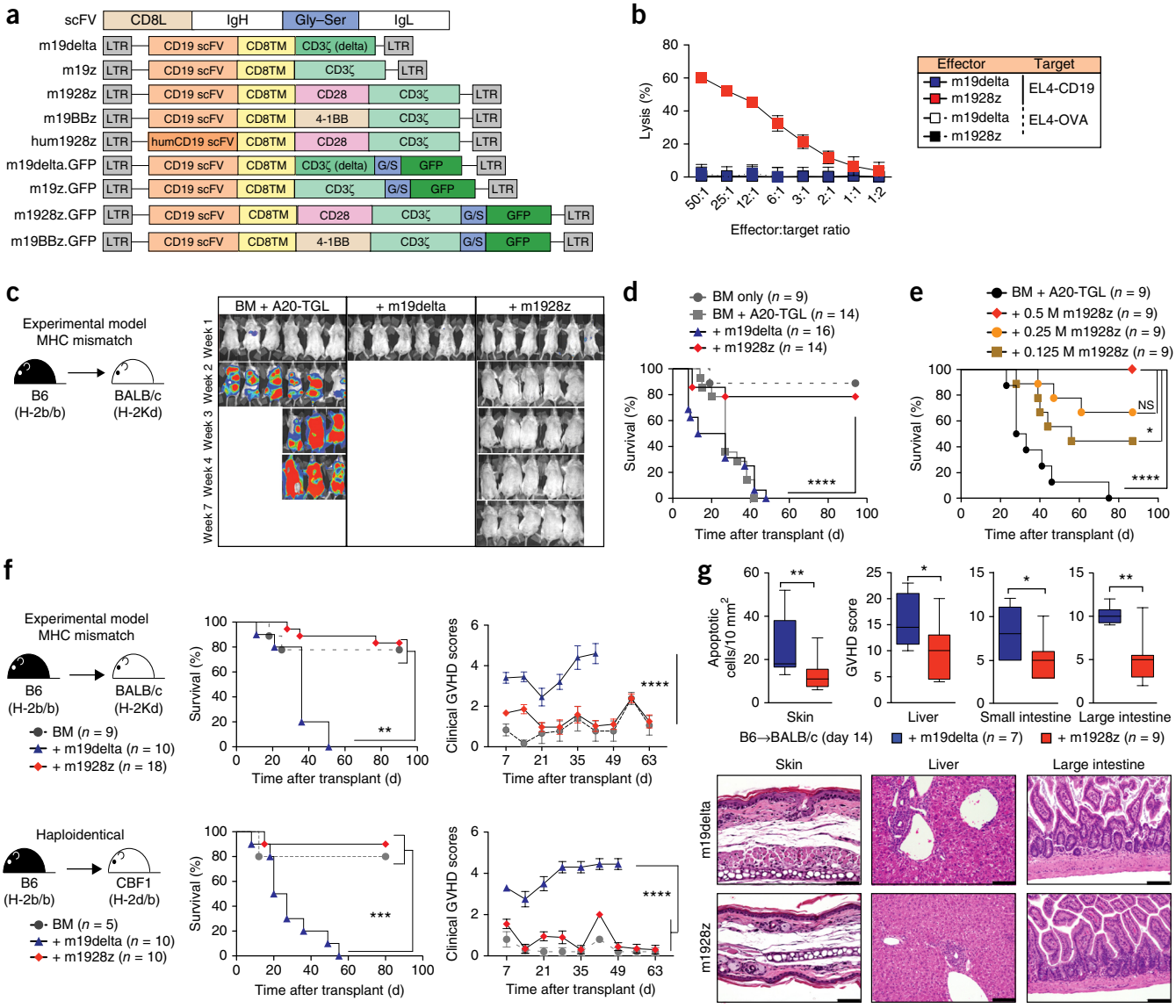

Figure 1 m1928z T cells eliminate CD19-expressing lymphoma cells while exerting significantly less GVHD activity. (**a**) Representation of the mouse CD19 CAR constructs: m19delta (mouse-specific CAR lacking functional ζ chain), m19z (mouse-specific functional CAR, no costimulation), m1928z (mouse-specific functional CAR, CD28 costimulation), m19BBz (mouse-specific functional CAR, 4-1BB costimulation), hum1928z (human-specific functional CAR, mouse CD28 costimulation), and m19delta.GFP and m1928z.GFP (CARs with GFP reporter). CD8L, mouse CD8 leader; CD8TM, mouse CD8 transmembrane region; Gly–Ser, glycine–serine linker IgH, immunoglobulin heavy chains. IgL, immunoglobulin light chains. (**b**) *In vitro* cytotoxicity assay using m19delta and m1928z CAR T cells as effectors and EL4-CD19 or EL4-OVA (control) cells as targets. Representative data from one of three experiments are shown. Lysis was performed with technical triplicate wells. In box-and-whisker diagrams, the median is shown with a horizontal line, the box extends from the 25th to the 75th percentile, and the whiskers extend from the smallest value up to the largest. (**c**,**d**) Lethally irradiated BALB/c recipients were reconstituted with B6 Lin-depleted BM cells and inoculated with A20-TGL lymphoma cells. Designated groups were treated with 1×10^6 B6 m19delta or m1928z T cells per mouse. (**c**) Tumor growth was monitored by *in vivo* bioluminescence. The bioluminescence images are from one of two experiments. (**d**) Survival was monitored for up to 100 d after transplantation. (**e**) Lethally irradiated BALB/c recipients were reconstituted with B6 Lin-depleted BM cells and were then inoculated with A20-TGL lymphoma cells. Designated groups were treated with 0.5×10^6, 0.25×10^6, or 0.125×10^6 B6 m19delta or m1928z T cells per mouse (M, million). Survival was monitored. Results for mice treated with B6 m19delta T cells are depicted in **Supplementary Figure 3** for simplicity. (**f**) Lethally irradiated BALB/c (top) and CBF1 (bottom) recipients were reconstituted with B6 Lin-depleted BM cells. Designated groups were treated with 1×10^6 B6 m19delta or m1928z T cells. Both survival and weekly clinical GVHD scores were monitored. (**g**) Skin, liver, small intestine, and large intestine were dissected from recipients on day 14 after transplantation. H&E sections were analyzed for GVHD with blinding to mouse treatment. Scale bars, 100 μm. Results in **f** and **g** were pooled from two independent experiments. Survival curves were analyzed with a Mantel–Cox (log-rank) test, and grouped comparisons were made using a Mann–Whitney *U* test or two-way ANOVA. Data represent means ± s.e.m. $^*P < 0.05$, $^{**}P < 0.01$, $^{***}P < 0.001$, $^{****}P < 0.0001$.

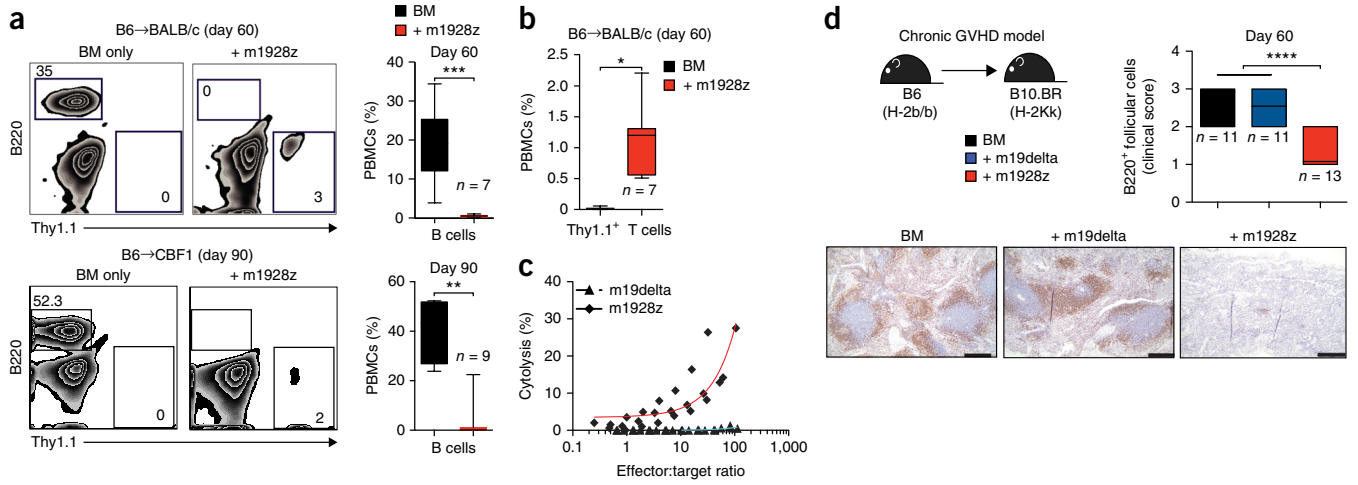

Figure 2 Allogeneic m1928z T cells mediate persistent B cell hypoplasia. (**a**–**c**) Lethally irradiated BALB/c or CBF1 recipients were reconstituted with B6 Lin-depleted BM cells. Designated groups were treated with 1×10^6 B6 m19delta or m1928z Thy1.1$^+$ T cells. (**a**) Peripheral blood was drawn at day 60 or day 90 after transplantation, and CD45-gated events were analyzed for B220$^+$ B cells by flow cytometry. (**b**) CD45$^+$Thy1.1$^+$ T cells were detected in peripheral blood. PBMCs, peripheral blood mononuclear cells. (**c**) Splenocytes were collected at day 14 after transplantation and used as effectors. ^{51}Cr-labeled EL4-CD19 cells were used as targets in an *in vitro* ^{51}Cr release cytotoxicity assay. The proportion of donor T cells in the spleen was determined by flow cytometry, and effective effector-to-target ratios are given. A representative plot from two independent experiments with similar results is shown ($n = 4$ mice/group, with lysis set up in triplicate). (**d**) B10.BR recipients were conditioned with cyclophosphamide on days 2 and 3, and TBI (total body irradiation; 7.5 Gy) was added on day 1. They were then reconstituted with 10×10^6 Lin-depleted BM cells. Designated groups were treated with 1×10^6 B6 m19delta or m1928z T cells. The size of B220$^+$ splenic follicles was scored after immunohistochemical staining. Pooled data from two independent experiments are depicted to the right, and representative micrographs are shown below. Scale bars, 200 μm. Comparisons were made using a Mann–Whitney *U* test or two-way ANOVA. Data represent means ± s.e.m.*$P < 0.05$, **$P < 0.01$, ***$P < 0.001$, ****$P < 0.0001$.

mortality rate similar to that with m19delta T cells. Finally, we assessed whether autonomous signaling from the CD28z cytoplasmic domain in the absence of antigen triggering was sufficient to protect against the occurrence of GVHD by comparing the extent of GVHD in recipients of hum1928z (**Fig. 1a**) versus m1928z T cells. Donor hum1928z T cells mediated GVHD that was significantly more lethal than that mediated by m1928z T cells, indicating that antigen-triggered signaling through the m1928z CAR is required for the suppression of GVHD (**Fig. 3h**).

To demonstrate the requirement for m1928z signaling in protection from GVHD, we used *Ighm*^{tm1Cgn} mice in which the gene for the immunoglobin mu heavy chain constant region (mu) is deleted (which lack mature B cells) as BM donors and *Rag2*-knockout BALB/c mice (which lack both mature T and B cell populations) as recipients (**Supplementary Fig. 8**). B6 m1928z T cells mediated significantly more mortality due to GVHD in *Rag2*-knockout BALB/c recipients of mu-deficient BM than in *Rag2*-knockout BALB/c recipients of B6 wild-type BM, suggesting that reduction of B cell number in hosts prevented m1928z-signaling-mediated protection from GVHD. We hypothesized that the mu-deficient reconstituted *Rag2*-knockout mice could still promote activation of m1928z signaling owing to the presence of CD19$^+$ pre-B cells in these mice[28]. Therefore, we used B6 *Cd19*-knockout donors to reconstitute BALB/c *Cd19*-knockout recipients, which lack the cognate antigen of the CD19 CAR[29]. CD19-deficient allo-HSCT recipients of CD19-deficient BM infused with B6 m1928z T cells demonstrated lethal GVHD levels similar to those found in recipients infused with B6 m19delta T cells (**Fig. 3i**). These data indicate that m1928z signaling in response to CD19$^+$ B cells is necessary for the inhibition of GVH responses.

The occurrence of GVHD is mediated by alloreactive TCR activation, and CAR-expressing alloreactive T cells likely experience concurrent stimulation via both the CAR and TCR in response to allogeneic B cells. To study the effect of CAR stimulation on TCR-directed killing, we generated a novel tricistronic vector, m1928z-OT-1, which promotes coordinated expression of m1928z and the OT-1 (OVA-specific) TCR (**Supplementary Fig. 9**). Polyclonal B6 m1928z-OT-1 T cells were tested as effectors against EL4 targets pulsed with the OVA peptide (EL4-OVA) in either the presence or absence of excess EL4-CD19 targets. Unlabeled and unpulsed EL4-CD19 (CAR-directed cold target) cells were added at 30-fold excess with respect to the amount of carboxyfluorescein succinimidyl ester (CFSE)-labeled EL4-OVA primary targets (TCR targets). The presence of EL4-CD19 target cells resulted in a significant reduction in the cytolysis of EL4-OVA targets mediated through the OT-1 TCR (**Fig. 4a**, left). TCR stimulation by targets pulsed with excess OVA also inhibited the killing of targets mediated by CAR signaling (**Fig. 4a**, right). This finding demonstrates that both the CAR and TCR can remain functional when simultaneously expressed and that activation of a T cell through one receptor can impair the lytic activity mediated by the other.

Chronic, repetitive activation of T cells via the endogenous TCR has been shown to result in anergy, exhaustion, and activation-induced cell death (AICD) in both chronic viral infection and tumor and self-antigen preclinical models[30]. Mouse models of dual-TCR-expressing T cells have demonstrated that T cells can be tolerized by chronic exposure to antigen, leading to their chronic exhaustion[31,32]. More recently, an exhaustion signature has been demonstrated in autonomously signaling GD2 CAR T cells that signal through the CD28 but not the 4-1BB costimulatory domain[27]. We studied these immunophenotypic markers of exhaustion in m1928z T cells after transplantation and found significantly higher expression of PD-1, LAG3, and Tim3 in splenic m1928z T cells from allo-HSCT recipients on day 14 after transplantation (**Fig. 4b**). While our findings suggest an exhaustion phenotype, these markers are also expressed in response to strong, chronic T cell activation. Therefore, we assessed signal

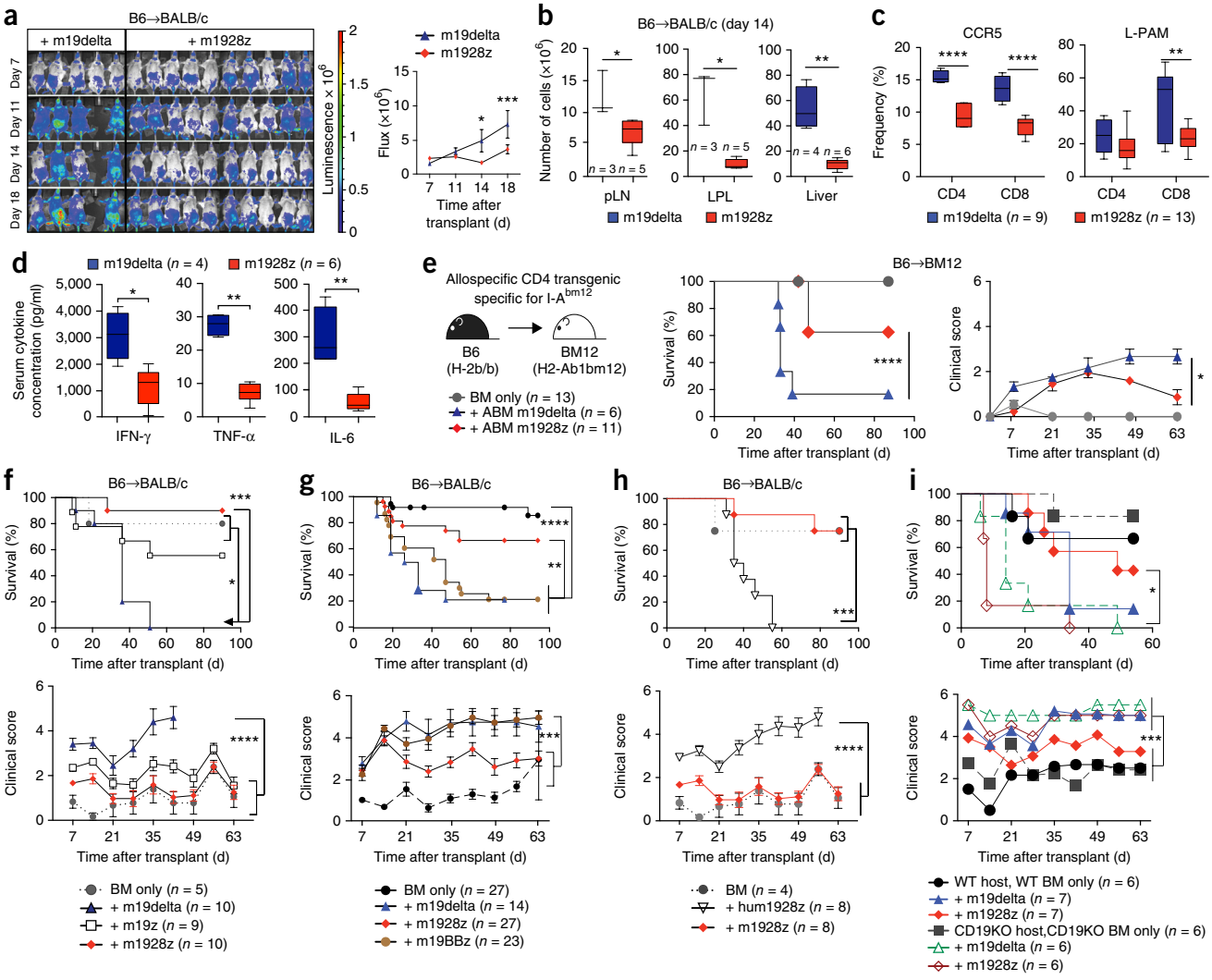

Figure 3 Allogeneic m1928z T cells exhibit decreased alloreactive proliferation and GVHD target organ infiltration. (**a**) Lethally irradiated BALB/c recipients were reconstituted with B6 Lin-depleted BM cells. Designated groups were treated with 1×10^6 luciferase$^+$Thy1.1$^+$ B6 m19delta or m1928z T cells. Bioluminescence imaging of the transplanted mice was performed weekly, and flux was measured. Data from one representative experiment and representing two independent experiments are shown. $n = 5$ for m19delta and $n = 10$ for m1928z T cells. (**b**–**d**) Lethally irradiated BALB/c recipients were reconstituted with B6 Lin-depleted BM cells. Designated groups were treated with 1×10^6 B6 m19delta or m1928z T cells. (**b**) Tissues were collected at day 14 after transplantation and homogenized. Cells were counted, and single-cell suspensions were analyzed by flow cytometry. The calculated numbers of donor Thy1.1$^+$ T cells in peripheral lymph node (pLN), lamina propria leukocytes (LPL), and liver are shown. Results are representative of one of two independent experiments. (**c**) Splenocytes were collected, and the proportions of cells expressing CCR5 and L-PAM were determined by flow cytometry. Pooled data from two independent experiments are depicted. (**d**) Cytokine expression in the serum was assessed at day 7 after transplantation with the Luminex multiplex assay. Data are from one of two independent experiments with similar results. (**e**) Lethally irradiated BM12 recipients were reconstituted with B6 Lin-depleted BM cells. Designated groups were treated with 2×10^5 ABM m19delta or m1928z T cells, and mouse survival and GVHD were monitored. (**f**–**h**) Lethally irradiated BALB/c recipients were reconstituted with B6 Lin-depleted BM cells. Designated groups were treated with 1×10^6 B6 m19delta, m1928z, and m19z (**f**), B6 m19delta, m1928z, and m19BBz (**g**), and B6 m19delta, m1928z, and hum1928z (**h**) T cells. Mouse survival and GVHD were monitored. Results are pooled from two independent experiments.(**i**) Lethally irradiated recipients (wild-type (WT) BALB/c or *Cd19*-knockout (CD19KO) BALB/c) were reconstituted with B6 or B6 *Cd19*-knockout Lin-depleted BM cells. Designated groups were treated with 1×10^6 B6 m19delta or m1928z T cells. Mouse survival and GVHD were monitored. Results are depicted from one of two independent experiments. Survival curves were analyzed with a Mantel–Cox (log-rank) test, and grouped comparisons were made using a Mann–Whitney *U* test or two-way ANOVA. Data in **b**–**i** represent means ± s.e.m.* $P < 0.05$, ** $P < 0.01$, *** $P < 0.001$, **** $P < 0.0001$.

transduction pathways in B6 m1928z T cells obtained from BALB/c transplant recipients on days 7, 10, and 14 after HSCT by analyzing TCR signaling using Phosflow analysis (**Fig. 4c**). We noted that there were significantly higher levels of phosphorylated protein kinase Cα (PKCα), ERK1 and ERK2 (ERK1/2), S6, STAT1, STAT3, and STAT5 present in donor m1928z T cells when compared to m19delta T cells. These results suggest that enhanced T cell stimulation in m1928z T cells arises as a consequence of stimulation via both the CAR and alloreactive TCR.

Next, we performed experiments to determine whether this enhanced T cell signal transduction produced a gene expression profile consistent with exhaustion or AICD. We adoptively transferred ABM T cells transduced with either the m19delta.GFP or m1928z.GFP vector (**Fig. 1a**) into BM12 recipients of B6 BM and then performed

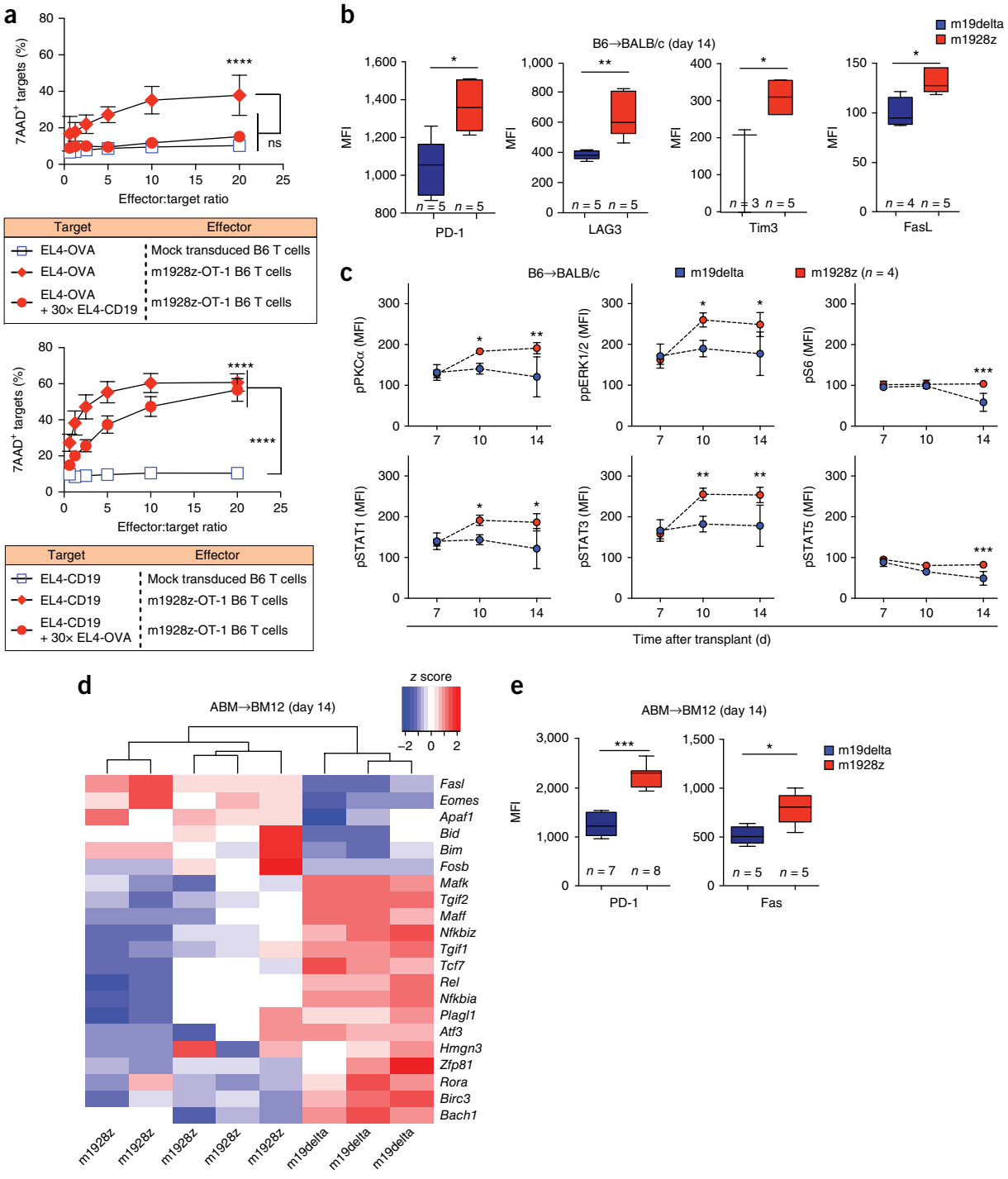

Figure 4 Alloreactive m1928z T cells are hyperactive and exhausted, and they undergo deletion. (**a**) m1928z-OT-1 T cells or mock-transduced T cells were used as effectors. Left, CFSE-labeled EL4 cells pulsed with OVA peptide (10 μM; SIINFEKL) were used as targets with or without non-labeled EL4-CD19 cells as cold targets. Right, CFSE-labeled EL4-CD19 cells were used as targets with or without unlabeled EL4 cells pulsed with OVA peptide (10 μM; SIINFEKL) as cold targets. Lysis at 5 hours was estimated as the percentage of 7AAD$^+$CSFE$^+$ targets out of the total number of CSFE$^+$ targets. Combined data from three experiments are shown ($n = 9$ (3 biological × 3 technical replicates)). Each data point reflects the average ± s.e.m. (**b**,**c**) Lethally irradiated BALB/c recipients were reconstituted with B6 Lin-depleted BM cells. Designated groups were treated with 1×10^6 Thy1.1$^+$ B6 m19delta.GFP or m1928z. GFP T cells. (**b**) Splenocytes collected at day 14 after HSCT were counted, and cell surface expression of exhaustion markers was measured on cells gated for Thy1.1 and GFP positivity. Data are representative of two independent experiments with similar results. MFI, mean fluorescence intensity. (**c**) Splenocytes were collected on designated days after HSCT, and the phosphorylation status of signaling proteins was evaluated in cells gated for Thy1.1 and GFP positivity. (**d**,**e**) Lethally irradiated BM12 recipients were reconstituted with B6 Lin-depleted BM cells. Designated groups were treated with 1×10^5 ABM m19delta.GFP or m1928z.GFP T cells. Splenocytes were collected at day 14 after HSCT. (**d**) Global transcriptional profiles of FACS-sorted GFP$^+$ CAR T cells. (**e**) Splenocytes were counted, and cell surface expression of exhaustion markers was measured on CAR T cells gated for GFP positivity. Data are representative of two independent experiments with similar results. Comparisons were made using a Mann–Whitney *U* test or two-way ANOVA. Data represent means ± s.e.m. $^*P < 0.05$, $^{**}P < 0.01$, $^{***}P < 0.001$, $^{****}P < 0.001$. ns, not significant.

transcriptome profiling on splenic GFP+ CAR T cells sorted at 14 d after transplantation from allo-HSCT recipients, an approach that ensured that only cells capable of receiving signals through both the TCR and CAR were included in the analysis (**Fig. 4d**). Microarray data were consistent with a population of T cells undergoing exhaustion and deletion, as evidenced by the upregulation of *Bim* (*Bcl2l11*), *Bid*, *Fasl*, *Apaf1*, and *Eomes*, as well as the downregulation of *Tcf7*, which is associated with progressive T cell differentiation and loss of self-renewal function[33,34]. Pathway analysis showed that the greatest differences between m1928z and m19delta T cells were in apoptosis pathways, especially those related to programmed cell death, caspase activation, and FasL signaling. We validated the array data by flow cytometry of GFP+ CAR T cells, confirming increased cell surface expression of Fas, along with the previously observed increase in PD-1 expression (**Fig. 4e**). These data suggest that alloreactive m1928z cells exhibit an increased level of cumulative T cell signaling in response to CD19 and alloantigens, leading to the chronic activation of these cells and their eventual functional exhaustion and programmed cell death.

Recent clinical studies have reported minimal incidence of GVHD in recipients of donor CD19 CAR T cells for treatment of B cell malignancies that had progressed after allo-HSCT[16,17]. In these studies, the donor 1928z T cells were infused in the post-transplantation setting without lymphodepletion before T cell infusion. One study also reported increased expression of PD-1 on donor-derived allogeneic CAR T cells[16], which is consistent with our data. Our data demonstrate that alloreactive CAR T cells undergo hyperactivation, exhaustion, and subsequent deletion mediated by CD28 costimulation and CD3ζ signaling in multiple GVHD models, which are characterized by different MHC disparities and alloreactive T cells. We also show that concurrent activation of the CD19-specific CAR and TCR can promote acute lytic exhaustion of dual-specificity T cells. Together, these results suggest that both acute and chronic stimulation of T cells via the m1928z CAR can negatively affect the responsiveness of T cells to antigen presented to the TCR, independent of TCR specificity.

These findings may explain results showing impaired activity of virus-specific CD19 CAR T cells, which would be expected to receive dual stimulation through their CAR and TCR *in vivo*[35]. Phase 1 clinical trial data suggest that, while donor-derived CD19-targeted and CAR-modified virus-specific T cells maintain activity against CD19+ targets when administered in the post-transplantation setting to patients with relapsed B cell malignancies, there may be an inverse correlation between T cell persistence and CD19+ cell count (for acute lymphoblastic leukemia (ALL) and chronic lymphocytic leukemia (CLL) as well as normal B cells)[35]. In this setting, T cell survival could be negatively affected by recurrent CAR activation by CD19 and the presence of alloantigens that were not eliminated by preinfusion chemotherapeutic lymphodepletion.

We show that the presence of CD19 antigen, on either mature B cells or tumor cells, is critical to provide protection from GVHD. When intended for management of minimal residual disease (MRD), adoptive transfer of 1928z T cells should thus be performed after a time frame of B cell recovery, the duration of which is transplant dependent[36].

In summary, our data provide mechanistic insight into recent clinical trial results demonstrating that allogeneic donor CD19-specific CD28z CAR T cells promote anti-lymphoma activity, with minimal occurrence of GVHD. Our results support a model in which alloreactive T cells expressing CD19-specific CD28z CARs undergo cumulative activation in response to dual-specificity TCR and CAR signaling, resulting in loss of T cell function and the possible deletion of these cells. These findings caution about the complexity of relying on multiple antigen receptors in clonal T cells. Our findings further demonstrate a requirement for the presence of CD19+ targets to mediate inhibition of the potential of m1928z T cells to cause GVHD and indicate that infusion with donor 1928z T cells in the post-transplantation setting may result in the lowest incidence of GVHD when these cells are infused after B cell recovery.

METHODS

Methods, including statements of data availability and any associated accession codes and references, are available in the online version of the paper.

Note: Any Supplementary Information and Source Data files are available in the online version of the paper.

ACKNOWLEDGMENTS

We are thankful to M. Sayegh (Brigham and Women's Hospital and Children's Hospital Boston) for ABM mice, R. Negrin (Stanford University) for the A20-TGL cell line, E. Campeau (University of Massachusetts) for pENTR1A, D. Vignali (University of Pittsburgh Medical Center) for mouse TCR OTI-2A.pMIG II, and P. Khavari (Stanford University) for LZRS-Rfa plasmid. We appreciate the help of J. White, LCP, RARC, the flow cytometry core facility, the integrative genomics core, and the computational biology core at MSKCC. We also appreciate the help of H. Poeck in critical reading of the manuscript. This research was supported by National Institutes of Health award numbers R01-HL069929 (M.R.M.v.d.B.), R01-AI101406 (M.R.M.v.d.B.), P01-CA023766 (M.R.M.v.d.B.), and R01-AI100288 (M.R.M.v.d.B.), LLS (M. Sadelain), the Lymphoma Foundation, the Susan and Peter Solomon Divisional Genomics Program, MSKCC Cycle for Survival, and P30-CA008748 MSK Cancer Center Support Grant/Core Grant. A.G. is a fellow of the Lymphoma Research Foundation. M. Smith received funding from an NIH Diversity Supplement (PA-16-288) under R01-AI100288-08S1, the M.J. Lacher Research Fellowship (The Lymphoma Foundation), and the American Society for Blood and Marrow Transplantation New Investigator Award. M. Smith and S.J. are supported under an NIH T32 grant (T32-CA009207). S.J. is also a Young Investigator Awardee from the Conquer Cancer Foundation of ASCO. M.L.D. is supported by an ASH-AMFDP career development award, the Damon Runyon Fund, and K08-CA148821 (NCI). J.L.Z. is supported by LLS TRP grant 6465-15 and K08-CA160659 (NCI). A.Z.T. is supported by a grant from the Imaging and Radiation Sciences (IMRAS) Program of MSKCC. The content is solely the responsibility of the authors and does not represent the official views of the National Cancer Institute or the National Institutes of Health.

AUTHOR CONTRIBUTIONS

A.G. and M.L.D. conceived the project. A.G., M. Smith, S.E.J., and M.L.D. contributed to the design of the experiments, supervised and conducted the experiments, generated the manuscript figures, and wrote the manuscript. E.V. and K.V.A. conducted the experiments and generated the manuscript figures. F.P. contributed to the performance of microarray analyses and interpretation of the data. A.C.F.M., G.F.M., and C.L. contributed to the performance of histological analyses and interpretation of the data. G.G., F.M.K., E.R.L., S.L., H.V.J., A.Z.T., L.T., L.F.Y., and K.T. assisted in conducting experiments. J.L.Z., J.A.D., R.R.J., A.M.H., and A.S. contributed to the design of the experiments and their analyses. M. Sadelain and M.R.M.v.d.B. supervised the project, contributed to the design of the experiments and their analyses, and wrote the manuscript.

COMPETING FINANCIAL INTERESTS

The authors declare competing financial interests: details are available in the online version of the paper.

1. Ho, W.Y., Blattman, J.N., Dossett, M.L., Yee, C. & Greenberg, P.D. Adoptive immunotherapy: engineering T cell responses as biologic weapons for tumor mass destruction. *Cancer Cell* **3**, 431–437 (2003).
2. Sadelain, M., Rivière, I. & Brentjens, R. Targeting tumours with genetically enhanced T lymphocytes. *Nat. Rev. Cancer* **3**, 35–45 (2003).
3. Gill, S. & June, C.H. Going viral: chimeric antigen receptor T-cell therapy for hematological malignancies. *Immunol. Rev.* **263**, 68–89 (2015).
4. Sadelain, M., Brentjens, R. & Rivière, I. The basic principles of chimeric antigen receptor design. *Cancer Discov.* **3**, 388–398 (2013).

5. James, S.E. *et al.* Antibody-mediated B-cell depletion before adoptive immunotherapy with T cells expressing CD20-specific chimeric T-cell receptors facilitates eradication of leukemia in immunocompetent mice. *Blood* **114**, 5454–5463 (2009).
6. Brentjens, R.J. *et al.* Eradication of systemic B-cell tumors by genetically targeted human T lymphocytes co-stimulated by CD80 and interleukin-15. *Nat. Med.* **9**, 279–286 (2003).
7. Sadelain, M. CAR therapy: the CD19 paradigm. *J. Clin. Invest.* **125**, 3392–3400 (2015).
8. Kochenderfer, J.N. *et al.* Chemotherapy-refractory diffuse large B-cell lymphoma and indolent B-cell malignancies can be effectively treated with autologous T cells expressing an anti-CD19 chimeric antigen receptor. *J. Clin. Oncol.* **33**, 540–549 (2015).
9. Kalos, M. *et al.* T cells with chimeric antigen receptors have potent antitumor effects and can establish memory in patients with advanced leukemia. *Sci. Transl. Med.* **3**, 95ra73 (2011).
10. Brentjens, R.J. *et al.* Safety and persistence of adoptively transferred autologous CD19-targeted T cells in patients with relapsed or chemotherapy refractory B-cell leukemias. *Blood* **118**, 4817–4828 (2011).
11. Brentjens, R.J. *et al.* CD19-targeted T cells rapidly induce molecular remissions in adults with chemotherapy-refractory acute lymphoblastic leukemia. *Sci. Transl. Med.* **5**, 177ra38 (2013).
12. Grupp, S.A. *et al.* Chimeric antigen receptor–modified T cells for acute lymphoid leukemia. *N. Engl. J. Med.* **368**, 1509–1518 (2013).
13. Davila, M.L. *et al.* Efficacy and toxicity management of 19-28z CAR T cell therapy in B cell acute lymphoblastic leukemia. *Sci. Transl. Med.* **6**, 224ra25 (2014).
14. Lee, D.W. *et al.* T cells expressing CD19 chimeric antigen receptors for acute lymphoblastic leukaemia in children and young adults: a phase 1 dose-escalation trial. *Lancet* **385**, 517–528 (2015).
15. Maude, S.L. *et al.* Chimeric antigen receptor T cells for sustained remissions in leukemia. *N. Engl. J. Med.* **371**, 1507–1517 (2014).
16. Brudno, J.N. *et al.* Allogeneic T cells that express an anti-CD19 chimeric antigen receptor induce remissions of B-cell malignancies that progress after allogeneic hematopoietic stem-cell transplantation without causing graft-versus-host disease. *J. Clin. Oncol.* **34**, 1112–1121 (2016).
17. Kochenderfer, J.N. *et al.* Donor-derived CD19-targeted T cells cause regression of malignancy persisting after allogeneic hematopoietic stem cell transplantation. *Blood* **122**, 4129–4139 (2013).
18. Davila, M.L., Kloss, C.C., Gunset, G. & Sadelain, M. CD19 CAR-targeted T cells induce long-term remission and B cell aplasia in an immunocompetent mouse model of B cell acute lymphoblastic leukemia. *PLoS One* **8**, e61338 (2013).
19. Ghosh, A. *et al.* PLZF confers effector functions to donor T cells that preserve graft-versus-tumor effects while attenuating GVHD. *Cancer Res.* **73**, 4687–4696 (2013).
20. Ghosh, A. *et al.* Adoptively transferred TRAIL$^+$ T cells suppress GVHD and augment antitumor activity. *J. Clin. Invest.* **123**, 2654–2662 (2013).
21. Bar, M. *et al.* Donor lymphocyte infusion for relapsed hematological malignancies after allogeneic hematopoietic cell transplantation: prognostic relevance of the initial CD3$^+$ T cell dose. *Biol. Blood Marrow Transplant.* **19**, 949–957 (2013).
22. Srinivasan, M. *et al.* Donor B-cell alloantibody deposition and germinal center formation are required for the development of murine chronic GVHD and bronchiolitis obliterans. *Blood* **119**, 1570–1580 (2012).
23. Jacoby, E. *et al.* Murine allogeneic CD19 CAR T cells harbor potent antileukemic activity but have the potential to mediate lethal GVHD. *Blood* **127**, 1361–1370 (2016).
24. Kochenderfer, J.N., Yu, Z., Frasheri, D., Restifo, N.P. & Rosenberg, S.A. Adoptive transfer of syngeneic T cells transduced with a chimeric antigen receptor that recognizes murine CD19 can eradicate lymphoma and normal B cells. *Blood* **116**, 3875–3886 (2010).
25. Jenq, R.R. *et al.* Regulation of intestinal inflammation by microbiota following allogeneic bone marrow transplantation. *J. Exp. Med.* **209**, 903–911 (2012).
26. Zhao, Z. *et al.* Structural design of engineered costimulation determines tumor rejection kinetics and persistence of CAR T cells. *Cancer Cell* **28**, 415–428 (2015).
27. Long, A.H. *et al.* 4-1BB costimulation ameliorates T cell exhaustion induced by tonic signaling of chimeric antigen receptors. *Nat. Med.* **21**, 581–590 (2015).
28. Hasan, M., Polic, B., Bralic, M., Jonjic, S. & Rajewsky, K. Incomplete block of B cell development and immunoglobulin production in mice carrying the μ MT mutation on the BALB/c background. *Eur. J. Immunol.* **32**, 3463–3471 (2002).
29. Rickert, R.C., Roes, J. & Rajewsky, K. B lymphocyte–specific, Cre-mediated mutagenesis in mice. *Nucleic Acids Res.* **25**, 1317–1318 (1997).
30. Wherry, E.J. T cell exhaustion. *Nat. Immunol.* **12**, 492–499 (2011).
31. Teague, R.M. *et al.* Peripheral CD8$^+$ T cell tolerance to self-proteins is regulated proximally at the T cell receptor. *Immunity* **28**, 662–674 (2008).
32. Schietinger, A., Delrow, J.J., Basom, R.S., Blattman, J.N. & Greenberg, P.D. Rescued tolerant CD8 T cells are preprogrammed to reestablish the tolerant state. *Science* **335**, 723–727 (2012).
33. Paley, M.A. *et al.* Progenitor and terminal subsets of CD8$^+$ T cells cooperate to contain chronic viral infection. *Science* **338**, 1220–1225 (2012).
34. Gattinoni, L. *et al.* Wnt signaling arrests effector T cell differentiation and generates CD8$^+$ memory stem cells. *Nat. Med.* **15**, 808–813 (2009).
35. Cruz, C.R. *et al.* Infusion of donor-derived CD19-redirected virus-specific T cells for B-cell malignancies relapsed after allogeneic stem cell transplant: a phase 1 study. *Blood* **122**, 2965–2973 (2013).
36. Small, T.N., Robinson, W.H. & Miklos, D.B. B cells and transplantation: an educational resource. *Biol. Blood Marrow Transplant.* **15** (Suppl.), 104–113 (2009).

ONLINE METHODS

Mouse HSCT, GVHD, and GVL models. We obtained female C57BL/6 (B6), C57BL/7.Thy1.1 (Thy1.1$^+$ B6), CBF1, B10.BR, BALB/c, and BM12 mice from the Jackson Laboratory. ABM transgenic mice[37] were provided by M. Sayegh (Brigham and Women's Hospital and Children's Hospital Boston) and had been backcrossed onto a B6 background for at least 20 generations. These mice were then crossed to mice on a *Rag1*-knockout background derived from the Jackson Laboratory, which had previously been backcrossed onto the B6 background for ten generations. The mice used for experiments were 6–9 weeks old. They were co-housed with three to five mice per cage in all experiments. Statistical methods were not used to determine sample size. Sample sizes were chosen based on estimates from pilot experiments and previously published results to power appropriately. Mouse HSCT experiments with an MHC-disparate model (B6→BALB/c) and a MHC-haploidentical model (B6→CBF1) have been used extensively by others as well as by us[19,20]. The chronic GVHD model (B6→B10.BR) has been described in detail previously[22]. T cells were generated from splenocytes, as outlined, and were injected via the tail vein at the time of allograft injection. Recipients were monitored daily for survival and were scored weekly on a 10-point scale in a blinded fashion for signs of clinical GVHD as described previously[38]. Mice with scores greater than 5 were euthanized. Blinded histopathological assessment of GVHD in the liver, small intestine, and large intestine was performed at Massachusetts General Hospital and the University of Florida as previously described[19].

In A20-TGL lymphoma experiments, mice received 0.5×10^6 tumor cells/mouse on day 0 in a separate injection or 10×10^6 tumors cells/mouse on day 7 intravenously. All studies were approved by the Memorial Sloan Kettering Cancer Center Institutional Animal Care and Use Committee under protocol 99-07-025.

CAR constructs and CAR T cell production. The CAR constructs and T cell production have been described previously[18]. The constructs include an scFv, composed of a mouse CD8 signal peptide, IgH rearrangement, glycine–serine linker, and IgL rearrangement. The scFv was fused to the mouse CD8 hinge, the transmembrane region, and mouse stimulatory domains, including mouse CD28 and/or mouse CD3ζ. The CAR construct was cloned into the vector backbone SFG, which is a Moloney murine leukemia virus (MMLV)-based retroviral vector[39]. The tricistronic m1928z-OT-1 retroviral construct was generated using standard cloning techniques. pENTR1A no ccDB (w48-1) was a gift from E. Campeau (Addgene plasmid 17398). Mouse TCR OTI-2A.pMIG II was a gift from D. Vignali (Addgene plasmid 52111). The m1928z construct was cloned into pENTR1A in frame followed by a sequence encoding the E2A self-cleaving peptide. The OT-I TCR α and β chains were separated by the T2A self-cleaving peptide. The tricistronic construct was recombined into the LZRS-Rfa vector using Gateway LR Clonase II Enzyme mix (Invitrogen). LZRS-Rfa was a gift from P. Khavari (Addgene plasmid 31601). For retrovirus production, Phoenix-E packaging cells were transfected with the retroviral vectors using Effectene transfection reagent (Qiagen), and viral supernatant was used for transduction. For CAR T cell generation, splenic T cells were activated with both hCD3/CD28 Dynabeads (Invitrogen) and IL-2 (R&D Systems). Spinoculations were performed twice with the viral supernatant[40].

***In vivo* bioluminescence imaging.** A20-TGL cells and T cells from luciferase-expressing mice (a gift from R. Negrin) were visualized using *in vivo* bioluminescence imaging systems (Caliper Life Sciences)[19]. The bioluminescent flux was analyzed using Living Image software, version 4.3 (Caliper Life Sciences).

***In vitro* cytolysis.** *In vitro* cytolysis of targets was determined by measuring ^{51}Cr release from labeled target cells as described previously[20]. For cold target inhibition assays, polyclonal B6 m1928z-OT-1 T cells were added at varying effector:target ratios to targets with or without secondary cold targets. The primary targets—EL4-CD19 cells or EL4 cells pulsed with 10 μM SIINFEKL (OVA) peptide (Invivogen)—were labeled with 0.5 μM CSFE (Molecular Probes) and added to 96-well plates at 10^4 targets/well. In cold target wells, a 30-fold excess of non-CFSE-labeled secondary targets was added. Target lysis was assessed by flow cytometry at 5 h to determine the percentage of 7AAD$^+$ targets (Molecular Probes).

Flow cytometry. Antibody staining of cultured T cells or tissues obtained from killed mice was performed at 4 °C with mouse Fc Block (eBioscience) in 1% FBS in PBS. Stained cells were washed once with 1% FBS in PBS before being processed through a five-laser BD LSR II flow cytometer (BD Biosciences). Flow cytometry of blood cells was performed with a lyse–no wash preparation. Briefly, 25 μl of retro-orbital or cheek blood was incubated with antibodies for 25 min at 4 °C. Afterward, FACS Lysing Solution (BD Biosciences) was added, and the cells were evaluated. All flow cytometry data files were analyzed with FlowJo software (Tree Star). Protein L, an immunoglobulin-binding protein that binds to the variable light chains of immunoglobulin without interfering with the antigen-binding site, was used to detect expression of the CAR[41]. For m1928z-OT-1 T cells, cells were stained with CD19-His (Sinobiological) followed by anti-His-PE staining (Miltenyi) to demonstrate CD19 CAR expression and were then stained with anti-Vα2-APC (clone B20.1, Pharmingen) and anti-Vβ5.1/5.2-FITC (clone MR9-4, Pharmingen) to detect the OT-1 TCR chains. The following concentrations or dilutions were used: protein L–biotin (Genescript, M00097), 1 μg/sample; streptavidin-PE (Pharmingen, 554061), 1,000× dilution; CD19-His (Sinobiological, 50510-M08H-20), 125 ng/sample; anti-His-PE (Miltenyi, 130-098-810), 10× dilution; vα 2 TCR-APC (eBioscience, 17-5812), 200× dilution; vβ 5.1, 5.2 TCR-FITC (Pharmingen, 553189), 200× dilution.

For Phosflow cytometry, transplanted mice receiving m19delta or m1928z CAR T cells were killed at 7, 10, and 14 d after transplantation. Immediately after euthanasia, spleens were dissected and homogenized over a 70-μm cell strainer. Cells were rinsed through the strainer with prewarmed RPMI-1640 medium containing 2% paraformaldehyde (PFA). After centrifugation, cells were resuspended in RPMI-1640 medium with 2% PFA and incubated at 37 °C for 10 min. Subsequently, cells were washed with PBS, resuspended in ice-cold methanol, and kept at −20 °C for 1 h. After washing with PBS, permeabilized cells were finally stained for CD90.1 and the following phospho-specific antibodies: PKCα Thr497, ERK1/2 Thr202/Tyr204, S6 Ser235/Ser236, STAT1 Ser727, STAT3 Tyr705, and STAT5 Tyr694 (BD Biosciences). The following amounts or dilutions were used: PKCα-APC (Pharmingen, 560140), 50 tests/1 ml; ERK1/2 (pT202/pY204)–Alexa Fluor 647 (Pharmingen, 612593), 50 tests/1 ml; S6 (pS235/pS236)–Alexa Fluor 647 (Pharmingen, 560434), 50 tests/1 ml; STAT-3 (pS727)–Alexa Fluor 647 (Pharmingen, 560190), 50 tests/1 ml; STAT-3 (pY705)–Alexa Fluor 647 (Pharmingen, 557815), 50 tests/1 ml; STAT-5 (pY694)–Alexa Fluor 647 (Pharmingen, 612599), 50 tests/1 ml; CD90.1-PE (Pharmingen, 554898), 1,000× dilution. CAR T cell phosphorylation status was evaluated in CD90.1$^+$GFP$^+$ cells.

Microarrays. Spleens were dissected on day 14 after transplantation and FACS sorted for GFP-expressing CAR T cells. Sorted T cells were placed in TRIzol reagent, and RNA was isolated. Microarray analysis was performed with the Affymetrix MOE 430A 2.0 array. Microarray data were processed using the standard R/Bioconductor packages: gcRMA (based on the robust multi-array average method) for quantification and normalization and the LIMMA empirical Bayes method for analysis of differential expression[42,43]. Hierarchical clustering was performed using the R hclust function with the Euclidean distance measure. A heat map was generated using the heatmap.2 function from the gplots R package.

Cytokine detection. Retro-orbital blood was collected from mice, and serum was prepared by centrifugation after blood clotting. Serum was incubated with a Milliplex multi-analyte panel for mouse cytokines (EMD Millipore) and analyzed on a Luminex 100 system.

Statistics. Survival curves were analyzed with a Mantel–Cox (log-rank) test, and grouped comparisons were made using a Mann–Whitney *U* test or two-way ANOVA. Calculations were performed using Excel (Microsoft) and Prism (GraphPad) software. Data represent means ± s.e.m. In box-and-whisker diagrams, the median is shown with a horizontal line, the box extends from the 25th to the 75th percentile, and the whiskers extend from the smallest value up to the largest. *P* values that were less than 0.05 were considered to be statistically significant.

doi:10.1038/nm.4258

Data availability. All microarray data generated are available at the Gene Expression Omnibus (GEO) under accession GSE85397.

37. Sayegh, M.H. *et al.* Allograft rejection in a new allospecific CD4$^+$ TCR transgenic mouse. *Am. J. Transplant.* **3**, 381–389 (2003).
38. Schmaltz, C. *et al.* T cells require TRAIL for optimal graft-versus-tumor activity. *Nat. Med.* **8**, 1433–1437 (2002).
39. Rivière, I., Brose, K. & Mulligan, R.C. Effects of retroviral vector design on expression of human adenosine deaminase in murine bone marrow transplant recipients engrafted with genetically modified cells. *Proc. Natl. Acad. Sci. USA* **92**, 6733–6737 (1995).
40. Lee, J., Sadelain, M. & Brentjens, R. Retroviral transduction of murine primary T lymphocytes. *Methods Mol. Biol.* **506**, 83–96 (2009).
41. Zheng, Z., Chinnasamy, N. & Morgan, R.A. Protein L: a novel reagent for the detection of chimeric antigen receptor (CAR) expression by flow cytometry. *J. Transl. Med.* **10**, 29 (2012).
42. Irizarry, R.A. *et al.* Exploration, normalization, and summaries of high density oligonucleotide array probe level data. *Biostatistics* **4**, 249–264 (2003).
43. Smyth, G.K. Linear models and empirical Bayes methods for assessing differential expression in microarray experiments. *Stat. Appl. Genet. Mol. Biol.* **3**, Article 3 (2004).